

Crystal structure and fluxional behaviour in solution of $[\text{Rh}_4(\text{CO})_6(\mu\text{-Me}_2\text{PCH}_2\text{PMe}_2)_3]^\dagger$

Katya Besançon,^a Tito Lumini,^a Gábor Laurency,^a Serena Detti,^a Kurt Schenk^b and Raymond Roulet^{*a}

^a Institut de chimie moléculaire et biologique, Ecole Polytechnique Fédérale de Lausanne, 1015 Lausanne, Switzerland

^b Institut de cristallographie de l'Université, BSP, 1015 Lausanne, Switzerland

Received 8th November 2002, Accepted 16th January 2003
First published as an Advance Article on the web 5th February 2003

$[\text{Rh}_4(\text{CO})_6(\mu\text{-Me}_2\text{PCH}_2\text{PMe}_2)_3]$, the first example of a hexasubstituted derivative of $\text{Rh}_4(\text{CO})_{12}$, has a ground state geometry in the solid state and in solution of C_s symmetry with four edge-bridging carbonyls and with each diphosphine ligand bridging one edge of the same Rh_3 face. The result is an imbalance of the formal electron count at two rhodium atoms. As observed by ^{13}C - and ^{31}P -NMR, the mobility of the ligands is restricted to one $\mu\text{-CO} \leftrightarrow \eta\text{-CO}$ site exchange which astonishingly does not average dynamically the electron count on all four metal atoms.

Introduction

The bulk of studies on the migration of carbon monoxide about the surface of tetrametallic d^9 carbonyl clusters have dealt with derivatives of $\text{Rh}_4(\text{CO})_{12}$,^{1–5} $\text{Ir}_4(\text{CO})_{12}$ and mixed Ir–Rh dodecacarbonyls,⁶ and with a few derivatives of $\text{Co}_4(\text{CO})_{12}$.⁷ All simple carbonyl clusters with two electron donor ligands have, in common, a tetrahedral metal core with three edge-bridging COs defining a 'basal face' and 9 terminal ligands or, alternatively, with 12 terminal ligands. The four metal atoms always have a formal 18 valence electron count, except for one isomer of $[\text{Rh}_4(\text{CO})_9(\mu_3\text{-1,3,5-trithiane})]^{8a}$ which has a butterfly structure and for $[\text{Ir}_4(\text{CO})_8(\mu_3\text{-tripod})\text{PPh}_3]^{8b}$ and $[\text{Rh}_4(\text{CO})_8(\mu_3\text{-tripod})\text{P}(\text{OEt})_3]^{8c}$ whose intramolecular dynamics have not been examined. Intramolecular site exchange usually takes place by a merry-go-round of 6 COs about one or several triangular faces, as in $\text{Rh}_4(\text{CO})_{12}$,^{2,4} and $\text{IrRh}_3(\text{CO})_{12}$,² or by a change of basal face in which one bridging CO remains unaffected, as observed in $[\text{Ir}_4(\text{CO})_{10}(\eta\text{-diarsine})]^{9}$ and $\text{Ir}_2\text{Rh}_2(\text{CO})_{12}$.¹⁰ There is good evidence that the former process is concerted with a kinetic profile keeping an 18 electron count on all metal atoms.² Shapley *et al.* have proposed that the latter process goes through a transition state with a triply bridging CO,⁹ and a positive value for the activation volume of the site exchange in $\text{Ir}_2\text{Rh}_2(\text{CO})_{12}$ is an argument in favour of such a transition state.^{6,11} Thus, if the ground state geometry of a carbonyl cluster obeys the 18 electron rule, the observed site exchange may involve a transition state which does not follow that rule.

It would be interesting to look at the opposite case: if the ground state geometry of a carbonyl cluster does not correspond to a formal 18 electron count on all metal atoms, does the site exchange dynamically average the electron density on more or on all metal atoms relative to the ground state? The technique used to examine site exchange being NMR, the chosen metal and donor atoms of the ligands should have isotopes with nuclear spin one half. To be fluxional and have an adequate ground state geometry, the chosen tetrahedral cluster should have terminal CO ligands and more than 3 bridging COs. One of the simplest metal cores could thus be $\text{Rh}_4(\mu\text{-CO})_4$ with a symmetry different from D_{2d} . $\text{Rh}_4(\text{CO})_{12}$ having three bridging COs and the latter being better π -acceptors than

terminal COs, a good donor ligand should be introduced in the cluster, preferentially bidentate to lower the probability of forming isomers of similar energies with respect to monodentate ligands. $[\text{Rh}_4(\text{CO})_5(\mu\text{-CO})_3(\mu\text{-Ph}_2\text{PCH}_2\text{PPh}_2)_2]$ and its analogous IrRh₃ cluster are fluxional, but all metal atoms have a formal 18 electron count.¹² We thus decided to use $\text{Me}_2\text{-PCH}_2\text{PMe}_2$ as bidentate ligand. Its small bite angle and smallest phosphorus cone angle among diphosphines should favour additional CO substitution, stabilise the bridging ones, and possibly lead to a cluster satisfying the above mentioned properties.

Results and discussion

Crystal structure of $[\text{Rh}_4(\text{CO})_6(\mu\text{-Me}_2\text{PCH}_2\text{PMe}_2)_3]$

$[\text{Rh}_4(\text{CO})_6(\mu\text{-Me}_2\text{PCH}_2\text{PMe}_2)_3]$ (1) was the single product of the reaction of $\text{Rh}_4(\text{CO})_{12}$ with three mole equivalents of bis(dimethylphosphino)methane in THF at room temperature (see Experimental). Good crystals could only be obtained by cooling a dichloromethane solution to -25°C and these crystals contained the solvate $1 \cdot \text{CH}_2\text{Cl}_2$. As they tend to lose CH_2Cl_2 molecules, the crystal structure was determined by X-ray diffraction at 130 K. A view of the molecular structure is presented in Fig. 1. The molecule has a plane of symmetry passing by the midpoint of the Rh2–Rh2a bond, atoms Rh1 and Rh3, the CO bonds at C1, C2, C3 and C5, and the methylene group at C8. The positions of equivalent atoms (labelled with letter a) are obtained by the symmetry operation $(x, y, z) \rightarrow (x, -y + 1/2, z)$. Bond distances and angles are reported in Table 1. The mean value of the Rh–Rh distances (2.732(3) Å) is longer than that of $\text{Rh}_4(\text{CO})_{12}$ (2.698(4) Å),¹ and the values of the Rh2–Rh2a (2.6154(6) Å) and Rh1–Rh3 (2.8864(6) Å) distances are significantly shorter and longer, respectively, than the mean value. Each bidentate ligand bridges one edge of the Rh1–Rh2–Rh2a face, but not with the same tilt. Atoms P1 and P3 are nearly in the plane of the Rh1–Rh2–Rh2a face which is perpendicular to the plane of symmetry (the values of the P1–Rh1–Rh2–Rh2a and P1–Rh1–Rh2–P3 torsion angles are -177.6 and 178.7° , respectively), but not P2 (-24.4° for P1–Rh1–Rh2–P2). The P2–Rh2 bond makes similar angles with the normal to the Rh1–Rh2–Rh2a (63.4°) and Rh2–Rh2a–Rh3 planes (64.3°). The three symmetrically bridging carbonyls C4, C4a and C5 are approximately in the plane of the Rh2–Rh2a–Rh3 face (5.0° for C5–Rh2–Rh3–Rh2a and 179.0° for C4–Rh2–Rh2a–C5). In contrast with the majority of Rh_4 carbonyl clusters, there is a fourth bridging CO labelled C2 which is not terminal on Rh3 but instead bridges the Rh1–Rh3 edge. The bridge is

[†] Electronic supplementary information (ESI) available: regression of the Eyring plot of $[\text{Rh}_4(\text{CO})_6(\mu\text{-Me}_2\text{PCH}_2\text{PMe}_2)_3]$ as measured by ^{13}C -NMR between 169 and 293 K in CD_2Cl_2 . ^{31}P -NMR spectra of $[\text{Rh}_4(\text{CO})_6(\mu\text{-Me}_2\text{PCH}_2\text{PMe}_2)_3]$ in CD_2Cl_2 at three different temperatures. See <http://www.rsc.org/suppdata/dt/b2/b210986g/>

Table 1 Bond lengths [Å] and angles [°] for **1**

Rh(1)–C(1)	1.879(2)	Rh(3)–C(2)	1.981(2)
Rh(1)–C(2)	2.076(2)	Rh(3)–C(3)	1.874(2)
Rh(1)–P(1)	2.3110(5)	Rh(3)–C(4)	2.0812(14)
Rh(1)–Rh(2)	2.7550(4)	P(1)–C(7)	1.8403(14)
Rh(1)–Rh(3)	2.8864(6)	P(2)–C(7)	1.850(2)
Rh(2)–C(4)	2.0634(13)	P(3)–C(8)	1.8369(11)
Rh(2)–C(5)	2.0695(14)	O(1)–C(1)	1.144(3)
Rh(2)–P(2)	2.2780(5)	O(2)–C(2)	1.185(2)
Rh(2)–P(3)	2.2411(5)	O(3)–C(3)	1.144(3)
Rh(2)–Rh(2a)	2.6154(6)	O(4)–C(4)	1.172(2)
Rh(2)–Rh(3)	2.6907(3)	O(5)–C(5)	1.184(2)
C(1)–Rh(1)–C(2)	176.57(8)	P(3)–Rh(2)–Rh(1)	157.906(11)
C(1)–Rh(1)–P(1)	88.35(3)	P(2)–Rh(2)–Rh(1)	96.275(14)
C(2)–Rh(1)–P(1)	90.09(3)	Rh(2a)–Rh(2)–Rh(1)	61.662(7)
P(1a)–Rh(1)–P(1)	126.10(2)	Rh(3)–Rh(2)–Rh(1)	64.002(13)
C(1)–Rh(1)–Rh(2)	88.61(5)	C(3)–Rh(3)–C(2)	101.95(8)
C(2)–Rh(1)–Rh(2)	94.41(5)	C(3)–Rh(3)–C(4)	98.61(4)
P(1a)–Rh(1)–Rh(2)	145.124(9)	C(2)–Rh(3)–C(4)	98.44(4)
P(1)–Rh(1)–Rh(2)	88.52(2)	C(4a)–Rh(3)–C(4)	152.77(7)
Rh(2a)–Rh(1)–Rh(2)	56.676(13)	C(3)–Rh(3)–Rh(2)	144.17(3)
C(1)–Rh(1)–Rh(3)	140.09(6)	C(2)–Rh(3)–Rh(2)	98.70(5)
C(2)–Rh(1)–Rh(3)	43.35(5)	C(4)–Rh(3)–Rh(2)	49.23(4)
P(1)–Rh(1)–Rh(3)	108.196(11)	C(4)–Rh(3)–Rh(2a)	106.96(4)
Rh(2)–Rh(1)–Rh(3)	56.917(5)	Rh(2)–Rh(3)–Rh(2a)	58.157(13)
C(4)–Rh(2)–C(5)	161.06(5)	C(2)–Rh(3)–Rh(1)	45.98(5)
C(4)–Rh(2)–P(3)	94.65(4)	C(3)–Rh(3)–Rh(1)	147.93(6)
C(5)–Rh(2)–P(3)	87.57(5)	C(4)–Rh(3)–Rh(1)	88.26(4)
C(4)–Rh(2)–P(2)	94.56(4)	Rh(2)–Rh(3)–Rh(1)	59.081(11)
C(5)–Rh(2)–P(2)	103.15(4)	O(1)–C(1)–Rh(1)	171.2(2)
P(3)–Rh(2)–P(2)	104.044(14)	O(2)–C(2)–Rh(3)	133.6(2)
C(4)–Rh(2)–Rh(2a)	110.27(4)	O(2)–C(2)–Rh(1)	135.7(2)
C(5)–Rh(2)–Rh(2a)	50.81(3)	Rh(3)–C(2)–Rh(1)	90.67(7)
P(3)–Rh(2)–Rh(2a)	96.283(9)	O(3)–C(3)–Rh(3)	178.4(2)
P(2)–Rh(2)–Rh(2a)	146.441(13)	O(4)–C(4)–Rh(2)	140.43(11)
C(4)–Rh(2)–Rh(3)	49.81(4)	O(4)–C(4)–Rh(3)	138.31(11)
C(5)–Rh(2)–Rh(3)	111.51(3)	Rh(2)–C(4)–Rh(3)	80.96(5)
P(3)–Rh(2)–Rh(3)	105.52(2)	O(5)–C(5)–Rh(2)	140.56(3)
P(2)–Rh(2)–Rh(3)	134.782(12)	Rh(2)–C(5)–Rh(2a)	78.38(6)
Rh(2a)–Rh(2)–Rh(3)	60.922(6)	P(1)–C(7)–P(2)	114.21(8)
C(4)–Rh(2)–Rh(1)	92.26(4)	P(3)–C(8)–P(3a)	115.43(10)
C(5)–Rh(2)–Rh(1)	79.34(4)		

Symmetry transformations used to generate equivalent atoms labelled a: $x, -y + \frac{1}{2}, z$.

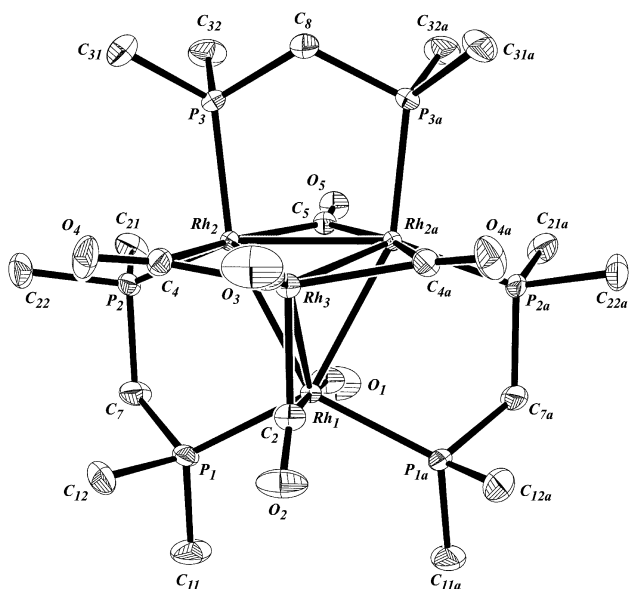


Fig. 1 Molecular structure of $[\text{Rh}_4(\text{CO})_6(\mu\text{-Me}_2\text{PCH}_2\text{PMe}_2)_3]$ at 130 K (ORTEP style plot at the 50 per cent level, hydrogen atoms omitted for clarity).

asymmetrical as the C2–Rh1 distance is significantly longer (2.076(2) Å) than C2–Rh3 (1.981(2) Å). The formal electron counts on Rh1 and Rh3 are 19 and 17, respectively, and cluster

1 has a structure satisfying one of the properties mentioned in the introduction.

Geometry of $[\text{Rh}_4(\text{CO})_6(\mu\text{-Me}_2\text{PCH}_2\text{PMe}_2)_3]$ in solution

The IR and NMR data of **1** indicate that the four carbonyl bridges are maintained in the ground state structure in solution. The ^{103}Rh -NMR spectrum (CD_2Cl_2 , 203 K, Fig. 2, right) exhibits three resonances at δ 4510, 3615 and 3025 ppm. The first has no Rh–P coupling and is assigned to Rh3. The third resonance is a triplet with one Rh–P coupling ($^1J = 137.7$ Hz) and is assigned to Rh1. The resonance at 3615 ppm is a *pseudo* triplet assigned to Rh2 and Rh2a which each couple with two distinct ^{31}P nuclei. The ^{31}P -NMR spectrum (CD_2Cl_2 , 203 K, Fig. 3 and 2, left) consists of three multiplets at δ –9.6, –14.6 and –35.3 ppm. Irradiation at the frequency of Rh1 does not affect the first two resonances but leaves that at –35.3 ppm as a doublet due to P–P coupling (Fig. 2, left). The latter is thus assigned to P1. Irradiation at the frequency of Rh2 does not affect the resonance of P1 but leaves those at –9.6 and –14.6 ppm as a doublet and a singlet, respectively. The doublet has the same coupling constant as that of P1 (117.5 Hz) and is assigned to P3. Only P1 and P3a (or P1a and P3) are in *pseudo trans* positions which are known to give higher coupling constants than phosphorus atoms in geminal positions.^{5,12} The structure indeed shows that the only value of P–Rh–Rh–P torsion angle close to zero or 180° is P1–Rh1–Rh2–P3 (178.7°), in contrast with the value of 149° for P1a–Rh1–Rh2–P2. Therefore, the same connectivity of P-atoms is observed as that in the solid.

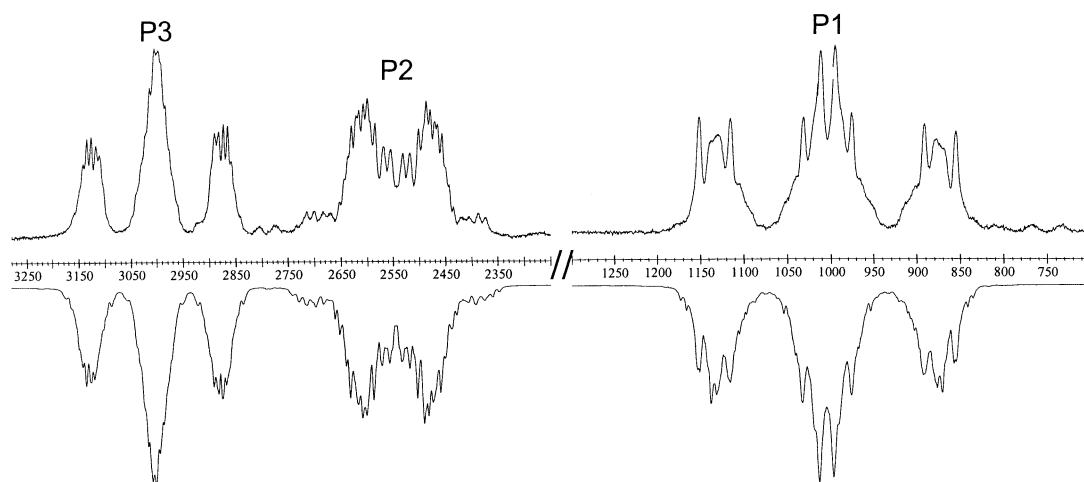


Fig. 3 Experimental and simulated ^{31}P -NMR spectra of $[\text{Rh}_4(\text{CO})_6(\mu\text{-Me}_2\text{PCH}_2\text{PMe}_2)_3]$.

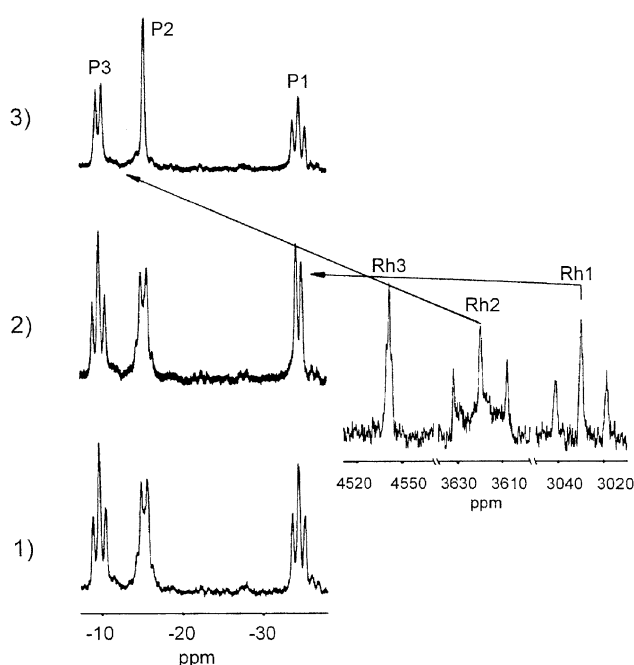


Fig. 2 ^{103}Rh -NMR (right) and ^{31}P -NMR (left, low resolution) spectra of $[\text{Rh}_4(\text{CO})_6(\mu\text{-Me}_2\text{PCH}_2\text{PMe}_2)_3]$ in CD_2Cl_2 at 203 K. (1) Without Rh decoupling, (2) and (3) decoupled as indicated by arrows.

No isomer of **1** is observed, in contrast with the analogous cluster $[\text{Ir}_4(\text{CO})_6(\mu\text{-Me}_2\text{PCH}_2\text{PMe}_2)_3]$ which exists as two isomers, one of which has each Ir-atom linked to two P-atoms as shown by X-ray crystallography.¹³ The spin system of **1** is too complex for complete simulation using the program gNMR¹⁴ (inverted spectrum in Fig. 3) as satisfactory iteration was obtained only for the major couplings (see Experimental).

The ^{13}C -NMR (CD_2Cl_2 , 169 K, Fig. 4, bottom) of a sample of **1** enriched in ^{13}CO (ca. 25%) shows 5 signals in the CO region with relative integrations 1 : 2 : 1 : 1 : 1 at δ 272.4 and 267.5 (2t, $J(\text{C-Rh})$ 31 Hz), 249.2 (t, $J(\text{C-Rh})$ 25 Hz), 210.7 (dt, $J(\text{C-Rh})$ 55.9, $J(\text{C-P})$ 21.8 Hz) and 203.3 ppm (d, $J(\text{C-Rh})$ 91.5 Hz). The two resonances with highest δ 's are clearly due to the 'normal' bridged carbonyls of the basal face Rh2–Rh2a–Rh3 as they show coupling with two ^{103}Rh nuclei with values of $J(\text{C-Rh})$ close to that observed in $\text{Rh}_4(\text{CO})_{12}$ (34 Hz).^{2,5} The resonances at 272.4 and 267.5 ppm are attributed to C5 and to C4, C4a on the basis of their relative integrations. The signal at 249.2 ppm is also a triplet and thus corresponds to C2, the fourth bridged carbonyl. The resonance at 203.3 ppm has no C–P coupling and is attributed to C3, the carbonyl bonded

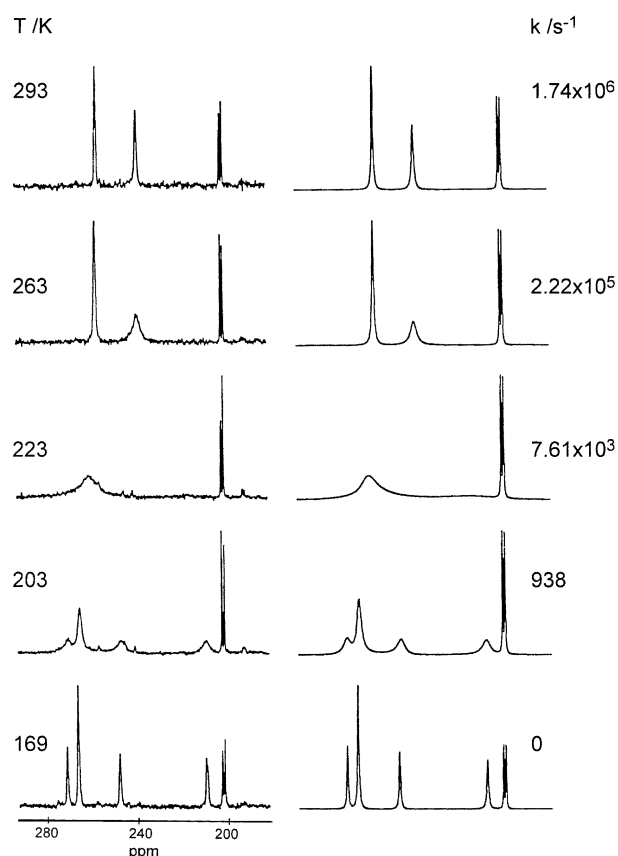


Fig. 4 Variable temperature ^{13}C -NMR spectra of $[\text{Rh}_4(\text{CO})_6(\mu\text{-Me}_2\text{PCH}_2\text{PMe}_2)_3]$ in CD_2Cl_2 . Left: experimental, right: calculated.

to the only rhodium atom without Rh–P connection. This assignment is in accordance with the higher value of $J(\text{C-Rh})$ observed for C3 (91.5 Hz) than for C1 (55.9 Hz). Indeed, in $\text{Rh}_4(\text{CO})_{12}$,^{2,5} a carbonyl ligand in a radial position (which has a position comparable to that of C3) has a higher value of $J(\text{C-Rh})$ (73.2 Hz) than that of a carbonyl in an apical position (61.0 Hz) with respect to the basal face (C1 is in an apical position with respect to the Rh1–Rh2–Rh2a face).

Site exchange in $[\text{Rh}_4(\text{CO})_6(\mu\text{-Me}_2\text{PCH}_2\text{PMe}_2)_3]$

A ^{13}C -EXSY spectrum (CD_2Cl_2 , 183 K, mixing time 100 ms, Fig. 5) shows the dynamic connectivities C1 \leftrightarrow C5 and C2 \leftrightarrow C4 (and C2 \leftrightarrow C4a by symmetry) while C3 does not exchange. The variable temperature ^{13}C -NMR spectra (CD_2Cl_2 , 169 to 239 K, Fig. 4) were then simulated using a 5 site exchange matrix with

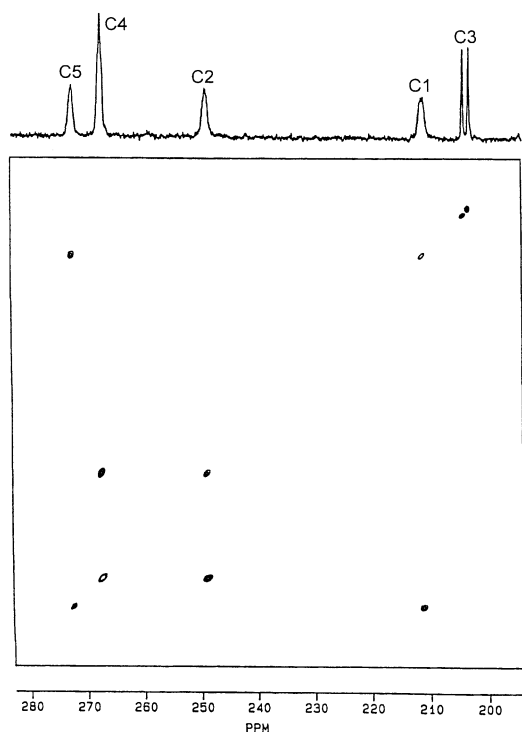


Fig. 5 ^{13}C -EXSY spectrum of $[\text{Rh}_4(\text{CO})_6(\mu\text{-Me}_2\text{PCH}_2\text{PMe}_2)_3]$ (CD_2Cl_2 , 183 K, mixing time 100 ms).

one rate constant k . Regression of the Eyring plot $\ln(k/T)$ vs. $1/T$ gave values of $39.3 \pm 1.2 \text{ kJ mol}^{-1}$ and $7.7 \pm 5.0 \text{ J K}^{-1} \text{ mol}^{-1}$ for ΔH^\ddagger and ΔS^\ddagger , respectively. At 298 K, $k = (2.1 \pm 0.3) \times 10^6 \text{ s}^{-1}$ and $\Delta G^\ddagger = 37.0 \pm 2.7 \text{ kJ mol}^{-1}$. The latter value is close to that obtained for the site exchange of carbonyls in $\text{Rh}_4(\text{CO})_{12}$ ($42.8 \pm 1.0 \text{ kJ mol}^{-1}$).² One may therefore propose that the fluxionality of **1** is due to site exchange of carbonyl ligands without concurrent Rh–P bond breaking. However, the mutual exchange $\eta\text{-C1} \leftrightarrow \mu\text{-C5}$ implies scrambling of the phosphorus atom positions. This indeed occurs as coalescence of the individual ^{31}P resonances at the averaged chemical shift is observed at 243 K (the spectra were not simulated as the size of the exchange matrix would have exceeded the capacity of the gNMR program). In the ground state of **1** the inequivalence of the phosphorus atom positions is best described by the values of the C3–Rh3–Rh–P torsion angles which are somewhat different (69.8° for P1–Rh1–Rh3–C3, 77.3° for P2–Rh1–Rh3–C3 and 51.8° for P3–Rh2–Rh3–C3 in the crystal structure). Since C3 does not exchange, phosphorus scrambling may be interpreted as a relative displacement of their positions (without Rh–P bond breaking) which averages the C3–Rh3–Rh–P torsion angles during the site exchange of the carbonyls.

The mutual exchange $\eta\text{-C1} \leftrightarrow \mu\text{-C5}$ implies debridging carbonyl C5 towards Rh2 (or the symmetrically equivalent debridging towards Rh2a) and bridging C1 on the Rh1–Rh2a edge (Rh1–Rh2, respectively). Comparing the final and initial configurations shown in Fig. 6 gives the following exchanges: C1 \leftrightarrow C5, C2 \rightarrow C4a, C3 \rightarrow C3, C4 \rightarrow C2, C4a \rightarrow C4, P1 \rightarrow P2a, P1a \rightarrow P3a, P2 \rightarrow P1a, P2a \rightarrow P3, P3 \rightarrow P1 and P3a \rightarrow P2. This result is in agreement with the observed site exchange which involves three metal atoms, but not the fourth one (Rh3). Debridging of carbonyl C2 towards Rh3 would result in a formal electron count of 18 on all metal atoms and lead to an isomer of **1**, but the latter is not observed. However, it may be noted that this 18 electron count is observed at the synthesis time scale for the parent cluster $[\text{Ir}_4(\text{CO})_6(\mu\text{-Me}_2\text{PCH}_2\text{PMe}_2)_3]$ which exists in solution as two isomers, each of which having three (but not four) edge-bridging carbonyls.¹³ It should also be noted that hopping of a P-atom from one metal atom to

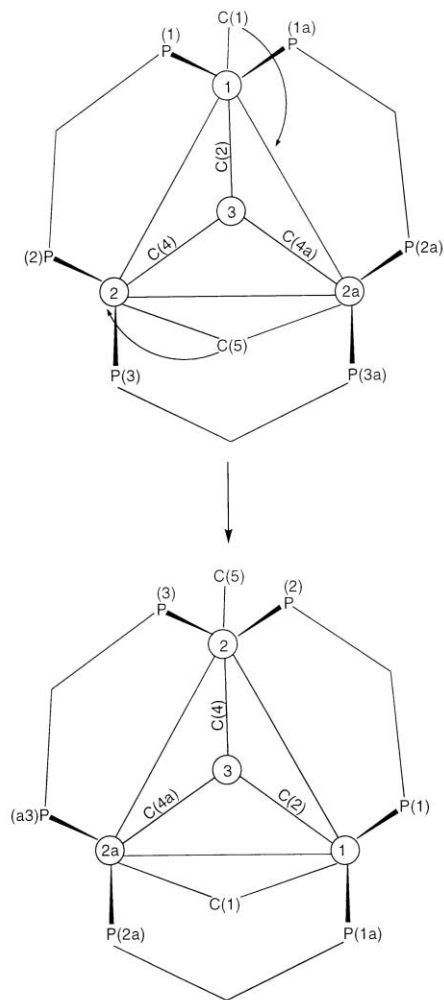


Fig. 6 Proposed mechanism for the carbonyl site exchange and phosphorus scrambling in $[\text{Rh}_4(\text{CO})_6(\mu\text{-Me}_2\text{PCH}_2\text{PMe}_2)_3]$ (numbers without letters represent rhodium atoms, all numbers correspond to those in Fig. 1, view of the tetrahedron along the Rh3–C3 direction with C3 on top of Rh3).

another could also average electron counts. Such a process occurs on the NMR time scale as a mutual exchange in $[\text{Rh}_4(\text{CO})_6(\mu\text{-PPh}_2)_4]$ ¹⁵ and as a non-mutual exchange in the isomerisation $[\text{Ir}_4(\text{CO})_{10}(\eta\text{-Ph}_2\text{PCH}=\text{CHPPH}_2)] \rightleftharpoons [\text{Ir}_4(\text{CO})_{10}(\mu\text{-Ph}_2\text{PCH}=\text{CHPPH}_2)]$,¹⁶ but is not observed in the present case.

In conclusion, $[\text{Rh}_4(\text{CO})_6(\mu\text{-Me}_2\text{PCH}_2\text{PMe}_2)_3]$ is an example of a cluster having in its ground state an imbalance of electron count on the four metal atoms and whose fluxional process leaves that formal count unchanged on one of the metal atoms. In more realistic terms than formal counts, the electron density of **1** which has C_s symmetry in its ground state dynamically evolves to C_3 symmetry (but not to T symmetry by non mutual exchange or isomerisation) on the NMR time scale.

Experimental

All manipulations were carried out under nitrogen atmosphere using standard Schlenk techniques. NMR spectra were recorded on a Bruker AC 200 (^1H at 200.13 MHz, ^{31}P at 81.02 MHz and ^{13}C at 50.32 MHz), Bruker WH 360 (^{13}C at 90.55 MHz) and a Bruker DRX 400 (^{31}P at 161.93 MHz, ^{13}C at 100.6 MHz) spectrometers. The chemical shifts (δ) are referenced to Me_4Si (^1H and ^{13}C), to external 85% H_3PO_4 (^{31}P), and to the spectrometer frequency (^{103}Rh). The ^{13}C and ^{31}P spectra were ^1H decoupled.

Synthesis

[Rh₄(CO)₆(μ-Me₂PCH₂PMe₂)₃] (**1**). Bis(dimethylphosphino)methane (165 μl, 1.02 mmol, Strem Chemicals) was added to a solution of Rh₄(CO)₁₂¹⁷ (0.34 mmol) in THF (150 ml) at -50°C. The low temperature is necessary to avoid extensive decomposition of [Rh₄(CO)₁₀(μ-Me₂PCH₂PMe₂)], the first intermediate formed which is thermally unstable, competing with further substitution of COs. The solution is then stirred at room temperature for 24 h. Partial evaporation of the solvent left a solid which was chromatographed on a column of silica gel (4 × 25 cm) using THF as eluent. The red-brown fraction was evaporated and slow crystallisation gave **1** as red-brown micro-crystals. Yield 171 mg (51%) (Found: C, 25.87; H, 4.54; P, 19.02. C₂₁H₄₀O₆P₆Rh₄ requires C, 25.53; H, 4.28; P, 18.81%). IR (CH₂Cl₂, 293 K): ν(CO) 1968sh, 1923vs, 1755vs, 1738sh. ³¹P-NMR (CD₂Cl₂, 203 K): -9.6 (m, J(P1-Rh1) 137.7, J(P1-P3) 117.5 Hz), -14.6 (m, J(P2-Rh2) 149 Hz), -35.3 ppm (J(P3-Rh3) 120.2 Hz). ¹³C-NMR: see text.

Crystal structure

An irregular, but roughly globular, dark-red crystal was placed on an Enraf-Nonius CAD4 diffractometer equipped with AgKα radiation (λ = 0.56086 Å). It was kept at T = 130(1) K in the nitrogen stream from an Oxford Cryostream. The lattice constants were determined from 25 reflections in the range 15° ≤ 2θ ≤ 38°. A hemisphere of intensities was measured as ω : 2θ scans of which the width was 0.6 + 0.45 tan(θ)°. The targeted σ(I)/I was 0.025, but the total scan time was limited to 150 s. The data were corrected for Lorentz and polarization effects, but an absorption correction was deemed unnecessary. The structure was easily solved with the help of DIRDIF97¹⁸ and refined by means of SHELX97.¹⁹ All non-hydrogen atoms were refined anisotropically, but the hydrogens were made to ride on their associated carbons and their IDP's were coupled to the latter.

Crystallographic data: C₂₁H₄₀O₆P₆Rh₄·CH₂Cl₂; M/g mol⁻¹ = 1070.92; T/K = 130(2); crystal system: orthorhombic; a = 17.340(4), b = 17.788(4), c = 12.037(2) Å, V = 3712.7(13) Å³, space group Pnma; Z = 4; μ(AgKα)/mm⁻¹ = 1.144; F(000) = 2104; θ scan: 1.61 to 26.97°; -17 < h < 28, -22 < k < 28, 0 < l < 19; reflections collected/unique 16348/8415; R_{int} = 0.0237; χ² on F² = 2.093; final R₁ = 0.021, wR₂ = 0.046 [I > 2σ(I)].

CCDC reference number 197240

See <http://www.rsc.org/suppdata/dt/b2/b210986g/> for crystallographic data in CIF or other electronic format.

Acknowledgements

We thank the Swiss National Science Foundation (grant 2000-652457.01) for financial support.

References

- 1 L. J. Farrugia, *J. Cluster Sci.*, 2000, **11**, 39.
- 2 K. Besançon, G. Laurency, T. Lumini, R. Roulet, R. Bruyndonckx and C. Daul, *Inorg. Chem.*, 1998, **37**, 5634.
- 3 B. F. G. Johnson and Y. V. Roberts, *Inorg. Chim. Acta*, 1993, **205**, 175; B. F. G. Johnson and R. E. Benfield, *J. Chem. Soc., Dalton Trans.*, 1978, 1554; F. A. Cotton, *Inorg. Chem.*, 1966, **5**, 1083.
- 4 J. Evans, B. F. G. Johnson, J. Lewis, J. R. Norton and F. A. Cotton, *J. Chem. Soc., Chem. Commun.*, 1973, 807.
- 5 B. T. Heaton, L. Strona, R. Della Pergola, L. Garlaschelli, U. Sartorelli and I. H. Sadler, *J. Chem. Soc., Dalton Trans.*, 1983, 248; B. T. Heaton, L. Longhetti, D. M. P. Mingos, C. E. Briant, P. C. Minshall, B. R. Theobald, L. Garlaschelli and U. Sartorelli, *J. Organomet. Chem.*, 1981, **213**, 333; B. T. Heaton, L. Longhetti, L. Garlaschelli and U. Sartorelli, *J. Organomet. Chem.*, 1980, **192**, 431.
- 6 R. Roulet in *The synergy between dynamics and reactivity at cluster and surfaces*, ed. L. J. Farrugia, NATO ASI Series, Kluwer Academic Publications, 1995, 465; and references therein. B. E. Mann, M. D. Vargas and R. Khadar, *J. Chem. Soc., Dalton Trans.*, 1992, 1725 and references therein.
- 7 C. Sizun, P. Kempgens, J. Raya, K. Elbayed, P. Granger and J. Rose, *J. Organomet. Chem.*, 2000, **604**, 27; P. Granger, K. Elbayed, C. Sizun, P. Kempgens, J. Raya and J. Rose, *J. Chim. Phys.-Chim. Biol.*, 1999, **96**, 1479; J. Evans, B. F. G. Johnson, J. Lewis, T. W. Matheson and J. R. Norton, *J. Chem. Soc., Dalton Trans.*, 1978, 626; M. A. Cohen, D. R. Kidd and T. L. Brown, *J. Am. Chem. Soc.*, 1975, **97**, 4408; A. Sisak, C. Sisak, F. Ungvary, G. Palyi and L. Marko, *J. Organomet. Chem.*, 1975, **90**, 77.
- 8 (a) R. J. Crowte, J. Evans and M. Webster, *J. Chem. Soc., Chem. Commun.*, 1984, 1344; (b) D. F. Foster, J. Harrison, B. S. Nicholls and A. K. Smith, *J. Organomet. Chem.*, 1983, **248**, C29; (c) J. R. Kennedy, P. Selz, A. L. Rheingold, W. C. Troglor and F. Basolo, *J. Am. Chem. Soc.*, 1989, **111**, 3615.
- 9 J. R. Shapley, G. F. Stuntz, M. M. Churchill and J. P. Hutchinson, *J. Chem. Soc., Chem. Commun.*, 1979, 219; A. Strawczynski, R. Ros, R. Roulet, F. Grepioni and D. Braga, *Helv. Chim. Acta*, 1988, **71**, 1885.
- 10 G. Bondietti, G. Suardi, R. Ros, R. Roulet, F. Grepioni and D. Braga, *Helv. Chim. Acta*, 1993, **76**, 2913.
- 11 G. Laurency and R. Roulet, unpublished results.
- 12 K. Besançon, PhD Thesis, University of Lausanne, Switzerland, 1996.
- 13 C. Hall, T. Lumini, K. Schenk and R. Roulet, unpublished results.
- 14 gNMR, version 4.1.2, Adept Scientific plc.
- 15 E. Gullo, S. Detti, G. Laurency and R. Roulet, *J. Chem. Soc., Dalton Trans.*, 2002, 4577.
- 16 G. Laurency, G. Bondietti, R. Ros and R. Roulet, *Inorg. Chim. Acta*, 1996, **247**, 65.
- 17 S. Martinengo, P. Chini and G. Giordano, *J. Organomet. Chem.*, 1971, **27**, 389.
- 18 P. T. Beurskens, G. Beurskens, W. P. Bosman, R. de Gelder, S. Garcia-Granda, R. O. Gould, R. Israël and M. M. Smits, The DirDif-96 System of Programs, Laboratorium voor Kristallografie, Katholieke Universiteit te Nijmegen, 1996.
- 19 G. M. Sheldrick, SHELXL-97. Program for the Refinement of Crystal Structures, Universität Göttingen, Germany, 1997.